Geosciences and Engineering, Vol. 13, No. 2 (2025), pp. 14–31.
https://doi.org/10.33030/geosciences.2025.02.002

OPTIMIZATION OF PETROPHYSICAL LABORATORY MEASUREMENTS

ROLAND DÓCS[1]*, KHALAT SHORSH MOHHAMED[2], HAZIM NAYEL ABDELFATTAH DMOUR[3], ZOLTÁN TURZÓ[4], KRISZTIÁN MÁTYÁS BARACZA[5]

[1]*Mining and Energy Institute of University of Miskolc, Hungary;
roland.docs@uni-miskolc.hu
[2]University of Miskolc, Hungary;
khalat.shorsh@gmail.com
[3] Mining and Energy Institute of University of Miskolc, Hungary;
hazin.dmour@uni-miskolc.hu
[4] Mining and Energy Institute of University of Miskolc, Hungary;
zoltan.turzo@uni-miskolc.hu
[5] Research Institute of Applied Earth Sciences of University of Miskolc, Hungary;
krisztian.baracza@uni-miskolc.hu
[1]https://orcid.org/0000-0002-1456-2990
[2]https://orcid.org/0009-0005-3276-400x
[4]https://orcid.org/0000-0002-7147-1163
[5]https://orcid.org/0000-0002-7809-9069

Abstract: Although petrophysical measurements in today's hydrocarbon industry are highly advanced and well-established, there remains considerable room for optimization, particularly in laboratory measurement techniques. While data acquisition methods in the field generally provide reliable and consistent results, the laboratory-based analysis of core and fluid samples often faces challenges related to measurement precision, standardization, and efficiency. Factors such as sample handling, preparation procedures, and the limitations of traditional experimental setups can introduce uncertainties that impact reservoir evaluation. By refining laboratory protocols, adopting advanced instrumentation, and integrating modern analytical methods, the accuracy and reproducibility of petrophysical laboratory measurements can be significantly improved, ultimately leading to better reservoir characterization and more effective resource management. In this context, the measurement procedures carried out at the Petrophysical Laboratory of the Institute of Applied Earth Sciences, University of Miskolc, were examined to optimize both the measurement methodology and the evaluation methods.

Keywords: *petrophysics, laboratory measurement, porosity, permeability*

1. INTRODUCTION

Petrophysical properties describe the physical and chemical characteristics of reservoir rocks that control the storage and movement of fluids within the pore space. These properties are essential for accurate reservoir characterization, production

forecasting, and field development planning. Several properties exist among which the most fundamental in regards of hydrocarbon production and storage are:

- **Porosity** – the fraction of the rock volume occupied by void spaces, determining the rock's capacity to store fluids.
- **Permeability** – a measure of the rock's ability to transmit fluids, controlled by pore size, shape, and connectivity.
- **Fluid saturation** – the relative proportions of oil, gas, and water occupying the pore space, which directly influences producible reserves.
- **Relative permeability** – in multiphase flow the relative value of each individual fluid permeability to the total rock permeability in function of saturation levels.
- **Grain density and bulk density** – key parameters for calculating porosity and for evaluating rock composition.
- **Pore-size distribution** – the ratio of volume occupied by each individual pore-size range in function of the total pore volume.
- **Capillary pressure** – the relationship between fluid distribution and pore-size, influencing hydrocarbon recovery efficiency.

While many of these properties can be estimated from well-logging tools, laboratory-based core analysis remains the most direct and precise method of determining them. Laboratory measurements allow for controlled testing conditions, standardized procedures, and calibration of well log-based interpretations. However, despite their importance, laboratory measurement techniques are often subject to limitations in precision, repeatability, and methodological consistency, which can affect the reliability of petrophysical evaluations.

In the laboratory of the Research Institute of Applied Sciences of the University of Miskolc several equipment are present capable of measuring most of these properties. The primary objective of this work was to optimize the porosity and permeability measurement procedures currently applied in the Institute, ensuring a more reliable characterization of properties in the future.

1.1. Theoretical background of porosity measurement techniques

Porosity as one of the most important basic parameters of rock material determines the ratio of the void volume to the total volume of the porous rock (Dotson et al. 1951). Consequently, it provides information about the maximum volume fraction that can be occupied by fluids in a given rock volume. From the various number of existing procedures (Lawrence and David, 2015) developed for the estimation/measurement of porosity the most reliable ones are still those performed in the laboratory. The determination of porosity relies on the combination of at least two volumetric (V_{pore}; V_{grain}; V_{bulk}) measurements (Anovitz and Cole, 2015). If either of the three volumes two are measured porosity can be calculated. However, several volume measurement procedures exist for all three cases, in laboratory circumstances the most likely used methods are the following:

- **Gravimetric (Archimedes) Method:** This technique is based on determining the bulk volume or grain volume of the sample through fluid displacement (Luffel and Howard, 1988). The bulk volume is measured by immersing the sample in a liquid of known density, while the grain volume is obtained after saturating the pores and accounting for fluid uptake. Porosity is calculated from the difference between the bulk and grain volumes.
- **Gas Expansion (Boyle's Law) Method:** This method uses the compressibility of a gas—often helium—to determine grain volume. The sample is placed in a chamber of known volume, and the gas is allowed to expand from a reference cell into the sample chamber (API, 1998). Applying Boyle's law, the grain volume is calculated, and porosity is obtained by subtracting the grain volume from the bulk volume. Helium is preferred due to its small molecular size, allowing it to penetrate very small pores and minimize adsorption effects.
- **Mercury Intrusion Porosimetry (MIP):** This technique measures pore volume and pore-size distribution (Jimmy et al., 2020) by forcing mercury into the pore spaces under controlled pressures. Since mercury is non-wetting to most rock minerals, it requires external pressure to penetrate the pores. According to the Washburn equation (Rapajic et al., 2025), the applied pressure is inversely related to the pore throat diameter. By incrementally increasing the pressure and recording the volume of mercury intruded, both total porosity and pore-size distribution can be determined. MIP is especially valuable for analyzing fine pore structures but is a destructive method and generally unsuitable for very friable or highly fractured samples.

In one of our previous works (Dócs and Szunyog, 2024) we already discussed the pros and cons of the most used combinations of volume measurements. In conclusion, suggesting the combination of a pore and grain volume measurement with the possibility of the lowest error. Where the procedure for grain volume measurement would be the two-chamber helium gas pycnometer due to its high accuracy, reliability and safety regarding sample integrity. For pore volume measurement unfortunately the altered form of gas pycnometer using a single chamber setup (Rajib et al. 2012) was not reachable in the Institute and the only solution at hand was the resaturation method (with water) was the only solution regarding the large cylindrical samples. This does not even remotely reach the same accuracy as the gas pycnometer. As a result, until today the Institute laboratory has relied on bulk volume measurements, using digital calipers.

Observing the possible equipment at hand we offered the solution of determining the porosity of only the small samples used for pore size distribution in MIP method. Since the grain volumes of these smaller samples could also be measured via the gas pycnometer at hand. With the two methods both the grain and pore volumes of these samples could be measured with the highest accuracy possible by modern day standards.

1.2. Theoretical background of permeability measurements

Permeability is a key property in materials science, geology, and engineering that describes how easily a fluid—such as water, oil, or gas—can flow through a porous material. Its importance lies in:

- **Groundwater and environmental studies** – It determine how quickly water moves through soil or rock, which is critical for groundwater recharge, contaminant transport, and water resource management.
- **Petroleum and natural gas extraction** – High permeability in reservoir rocks allows hydrocarbons to flow more efficiently to wells, influencing production rates and economic viability.
- **Civil engineering and construction** – Knowledge of soil permeability helps in designing drainage systems, foundations, and flood prevention measures.
- **Agriculture** – Soil permeability affects irrigation efficiency, root growth, and plant health.
- **Filtration and barrier design** – Controlling permeability is essential in making membranes, filters, and liners that either allow or restrict fluid passage.

In summary, permeability links material structure to fluid movement, making it a fundamental factor in predicting and controlling how natural and engineered systems behave. Since permeability is the parameter of the porous material it is independent of the flowing fluid if it is considered as non-damaging for the material.

Therefore, in theory, it can be measured using either liquids (usually water or brine solution) or gases after using Klinkenberg's slip correction (Jiang et al., 2024) as many have suggested in the past. However, many researchers pointed out that Klinkenberg corrected liquid permeability, usually overestimating the true measured values (Tanikawa and Shimamoto, 2009). In some more rare cases even underestimate those, although most researchers state that this is usually the case for tighter or more unconventional rock types there were others proving it at higher permeability samples (Tanikawa and Shimamoto, 2009). In any case, although the technique of permeability measurement using both gas and liquid is considered as well refined, procedures, if not done correctly, could result in extremely high errors.

For this reason, in the Institute for all sample plugs both permeability for gas and for brine solutions were always measured for samples of permeability above 10 mD.

2. MATERIALS AND METHODS

2.1. In search of the best porosity measurement solutions

As mentioned previously for large symmetrical samples the combination of gas pycnometry and geometric volume measurement was used in the past at the Institute. For this purpose, a Quantachrome Ultrapycnometer 1200e helium gas pycnometer was used as the main instrument. The device with the combination of geometric measurements using digital calipers for highly symmetrical large porosity samples had mostly shown high accuracy in the case of conventional rock materials. For unconventional samples on the other hand where porosity values were below ~5 % the accuracy of the bulk volume measurements induced major errors in the calculated porosity values. In some cases, at even lower values negative porosity could occur where the bulk volume was measured lower than the actual grain volume. This led to the conclusion that for such tight rocks the porosity of the large cylindrical samples was not tested due to no accurate solution at hand.

The only other installed porosimeter in the laboratory was a Quantachrome Pore Master 60GT series MIP which was mainly used for pore size distribution characterization of small cubic or amorphous samples produced from the offcuts of the large cylindrical samples. Although the MIP device could measure the pore volume directly with high accuracy, it was never truly used for porosity measurement because to do so the equipment required the bulk volume of the small sample to be measured. Although in the past they were done by digital calipers they were discarded due to their uncertainty regarding the large samples. There were some attempts in the past measuring the bulk volume by gravimetric method using mercury and relying on weight measurements (sample, empty dilatometer, sample + dilatometer and dilatometer full of mercury, finally sample + mercury + dilatometer) as described by the Archimedes' law and implemented in the devices software but were discontinued due to their tedious nature. Consequently, the measured data were only used in the form of intruded volumes and not porosity.

Observing the possibilities at hand, our suggestion was that the gas pycnometer should still be used for the grain volume consequently true density measurement of the large samples but in the absence of any accurate bulk or pore volume measurement method should not be used for porosity determination. For the small samples on the other hand the grain volume should be used for porosity determination in combination of the MIP procedure while the grain density could give a comparison with the large sample as well.

Providing the most sufficient and reliable volumetric combination for porosity and pore structure determination mentioned in the literature using those processes available in the Institute.

2.2. In search of the best permeability measurement processes

However steady state methods for both gas and fluid permeability (k) are well refined hence considered as rather simple procedures, if not done correctly could

result in significant errors. Also as discussed previously the uncertainties in slip corrected gas and true fluid permeability correlation are a critical factor.

Consequently, the permeability value of both gas and brine were always measured by the Institute on all cylindrical samples assuring the highest accuracy possible. Despite the well-established conditions some improvements could still be made.

2.2.1. Gas permeability procedure

The custom nitrogen gas permeability device was found to be most sufficient and was validated by a Core Lab Ultra-Perm 610 gas permeameter resulting in average errors well below 5 % at its current state.

When observing the evaluation process used by the Institute it was found that for dynamic viscosity (μ) calculation in function of temperature (T_{lab}) an empirical equation was used (equation 1) of which exact origin was not known but after further research was assumed to be a possible alteration of Sutherland's formula (equation 2), where the constant value of 111 resembled the S_μ effective temperature determined by Sutherland but for air not nitrogen

$$\mu_{Temp.} = 0{,}0177387 * \left[\frac{0{,}555*540{,}99+111}{0{,}555*(T_{lab}*9/5)+111}\right] * \left[\frac{T_{lab}*9/5}{540{,}99}\right]^{3/2} \quad (1)$$

We therefore suggested the switch of the formula in use to Sutherland's version for better clarity reasons. Therefore, we suggested a test to determine dynamic viscosity using both equations

$$\mu_{Sutherland} = \mu_0 * \left(\frac{T_{lab}}{T_0}\right)^{3/2} * \left(\frac{T_0+S_\mu}{T_{lab}+S_\mu}\right) \quad (2)$$

With the Sutherland's formula a technical question has risen, could compressed air be used for measurements instead of nitrogen in the permeameter developed by the Institute. This if proven accurate, would decrease the cost of measurement by eliminating the nitrogen consumption entirely (Mohammed, 2025).

For testing ten samples were chosen for gas permeability measurement with both air and nitrogen. First the nitrogen measurements were performed in the instrument after which the canister was switched for compressed air supplied by an oil less compressor. In both cases the same rotameter was applied that was used in the past for all nitrogen measurements and was validated by the Core Lab Ultra-Perm 610 instrument.

2.2.2. Liquid permeability procedure

Although the equipment and procedure of liquid permeability measurement is rather similar and relies on the pressure drop detection at constant flow conditions it differs to gas measurement by applying only one single injection rate rather than multiple ones. During gas measurement multiple runs are important since at higher

pressure differences gas will be increasingly compressed. During liquid measurement, however due to the incompressibility of the fluid this is not the case.

Fluid permeability measurements usually rely on a single injection pressure (or rate) during the entirety of the measurement. Permeability is then calculated as the average of the points at stable flow conditions. However, it is important that the injection flow rate is chosen wisely due to the criteria of laminar flow condition described by Darcy's law. If the preset flow rate reaches a certain value the developed flow will result in turbulent nature where Darcy's law will not apply. Hence in all cases the flow rates used for the measurements must be tested for the different permeability rocks to avoid turbulent flow.

Testing the flow conditions are relatively easy and could be performed by plotting the Darcy velocity (v) in function of the pressure gradient (∇p) at multiple injection rates as presented in Figure 1 (Singh et al., 2024). Laminar flow conditions are present where a laminar correlation is found between the plotted values. Here the slope of the linear function presents the ration of dynamic viscosity and the permeability (Equation 3) which are constant during isothermal conditions. In the past such tests were performed in the Institute and the optimal injection rate for such permeability rock was found to be 100 ml/h

$$v = \frac{k}{\mu}\nabla p \tag{3}$$

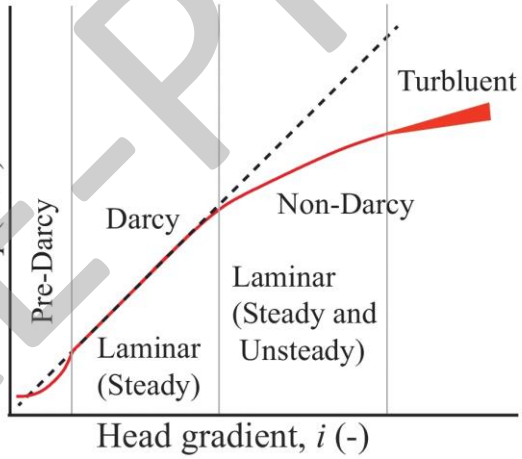

Figure 1

Flow regimes according to the velocity and pressure gradient values (Singh et al., 2024)

Although the single speed volumetric flow method for liquid permeability is mostly used in the industry it does not always represent the whole picture. If the porous material is homogeneous in nature, permeability during the darcy region usually shows a constant value. In some cases, however, where complex porous networks are present, the permeability will increase despite the linearity (Moghadam

and Chalaturnyk, 2014) presented also by a previous publication (Dócs et al., 2025). The phenomenon is related by the restriction in pore throats holding back flow in sections of the material. Where the driving force does not exceed the capillary force.

In shorter terms as flow rate increases, more volume of the porous material contributes to flow presenting as an increase in permeability during laminar conditions. Therefore, we performed measurements on three samples where permeability at multiple flow rates were tested covering a higher range than was performed in the past by the Institute. In the measurements the applied flow rates were chosen so that both conditions before and after the previously mentioned optimal flow rate (100 ml/h) could be tested. Therefore, measurements on the three samples were performed at flow rates of 5, 10, 20, 25, 50, 100, 200, 300, and 400 ml/h.

3. RESULTS AND DISCUSSION

3.1. Optimization of porosity measurement protocol

After the best combination was found, an investigation of both the helium pycnometry and MIP measurements for optimization purposes was carried out. All possible improvement possibilities regarding measurement conditions and data evaluation were taken into consideration. We found that regarding gas pycnometry no further possibilities for optimization were found in the institute's measurement protocol. Whereas for the MIP we found that several adjustments could be made to improve the measurement process:

- Measurement of true mercury column height after low-pressure procedure for correction in true mercury column weight acting on the pore space for improved penetration calculation data before high-pressure measurement.
- Setting the "Print one out of every …. data points." from the default 10 to 1 for better data set generation.
- Altering the default "Global Reduction Data Parameters" (pore radius to diameter, intrusion pressure from PSI to Pascal, unit of pore size from Angstroms to Microns).
- Changing the "Mode calculated from" option from dX(dr) to dX(dlog) of which is the preferred as many authors suggest.

Although the previous settings had made significant improvements in data generation, we found a huge limitation regarding the analysis capabilities in the equipment's software. Unfortunately, the developer had not made it in mind for data analysis purposes. The operator, however, has the possibility of choosing from an enormous amount of preset data tables and graphs, these are for only display purposes and do not have the option for direct data export. In addition, due to data formatting and the limitations of EXCEL data copying the data could not be transferred directly into .xlsx format.

However, through trial and error, a manual solution for data export was found, allowing all necessary intrusion data to be imported into .xlsx format. Afterwards, based on literature and personal experience, an evaluation sheet was made (Figure

2) capable of not only displaying the required graph combinations but also calculating and visualizing (adjustable) user-defined pore size ranges and their contribution to the total pore structure, while also capable of calculating the mode pore diameter of the sample. Providing a much more reasonable solution for data analysis than what was obtainable using the factory software of the MIP device.

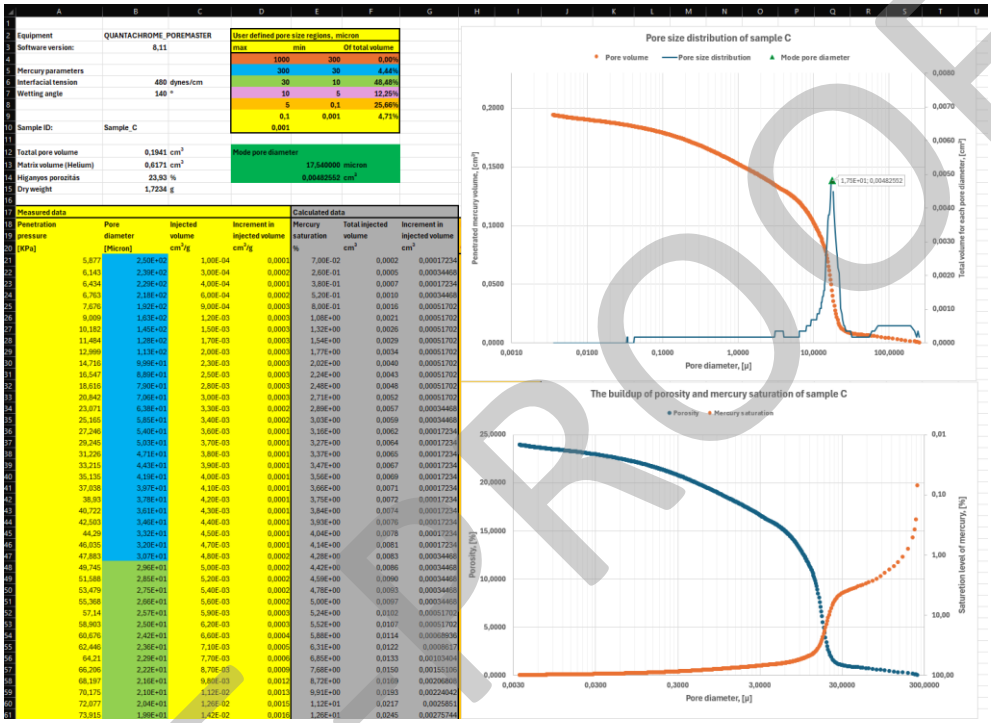

Figure 2

Screenshot of the newly developed MIP data analyzing excel sheet

Table 1

Pore size distribution of the chosen samples

	Sample A	Sample B	Sample C
Mode pore diameter (μm)	16,73	16,36	19,24
Porosity (%)	23,93	25,82	24,30
Pore size range 1000-300, %	0,0000	0,0000	0,0000
Pore size range 300-30, %	4,4395	4,9643	7,0189
Pore size range 30-10, %	48,4789	59,1777	42,2008
Pore size range 10-5, %	12,2529	8,8254	7,7207
Pore size range 5-0,1, %	25,6601	21,6696	34,3046
Pore size range 0,1-0,001, %	4,7058	1,8912	6,0538

The new Excel sheet was used to characterize the pore structure of 3 samples (Table 1) which were chosen for the liquid permeability measurement due to their

almost exact pore range stats. The percentage of each pore size range was calculated as the ratio of the cumulative volume occupied by all pores within the given range to the total pore volume.

3.2. Optimization of gas permeability measurement protocol

3.2.1. Dynamic viscosity

Sutherland's equation is a widely used one for its reliability and efficiency therefore after testing it at a temperature range usually present during measurements, we suggested it rather than the one permanently used due to the less than 1 % error rate (Table 2). The constants in the formula were T_0 (273), μ_0 (1,663*10^{-5}) and S_μ (107).

Table 2

Difference between the two viscosity formulas

Temperature [C°]	Original [mPa s]	Sutherland [mPa s]	Error [%]
20,0	0,017400407	0,017572919	0,9914
20,2	0,017409604	0,017582118	0,9909
20,4	0,017418798	0,017591313	0,9904
20,6	0,017427989	0,017600506	0,9899
20,8	0,017437177	0,017609696	0,9894
21,0	0,017446362	0,017618882	0,9889
21,2	0,017455544	0,017628066	0,9884
21,4	0,017464723	0,017637247	0,9878
21,6	0,017473899	0,017646424	0,9873

As predicted, the calculated dynamic viscosity values for the tested temperature region were almost a par with an absolute error of < 1 %. Although due to the unknown origin of the equation we still recommend Sutherland's formula for future use.

3.2.2. Measuring gas

Although rotameters are always calibrated for a single gas if two or more gases characteristics are similar, the same rotameter can be used if the correct constant for the gas is determined.

The reason why Sutherland's formula could be used for air although being a gas mixture is that both nitrogen and oxygen bear similar molecular properties (weight, collision diameter, intermolecular force characteristics) hence the individual viscosity-temperature relationships of both gases are close enough that the mixture behaves as of a single "effective" gas.

Explaining why the rotameter factory calibrated for air (with an original constant of 1,5) could be used sufficiently with nitrogen (laboratory calibrated constant of 1,317) in the past. After the rotameter was recalibrated for air the flow constant of 1,3 was found accurate. The difference in the factory and laboratory calibration was

dedicated to the wear of the instrument. The results for both absolute permeability and Klinkenberg corrected permeability measurements measured with air and nitrogen using Sutherland's viscosity formula are shown in Table 3.

Table 3

The error between nitrogen and air permeability values

Sample ID	Nitrogen		Air		Air/N2	Air/N2
	k_a mD	k_∞ mD	k_a mD	k_∞ mD	k_a %	k_∞ %
A	328	184	312	172	4,7339	6,3456
B	240	123	289	120	20,6381	2,1926
C	327	123	328	131	0,3508	5,9719
D	240	201	241	183	0,5611	8,5497
E	323	277	312	162	3,4392	41,2995
F	338	236	333	235	1,4330	0,5696
G	249	143	257	144	3,3101	1,2131
H	254	157	255	156	0,3159	0,2578
I	261	160	264	158	1,4668	1,4073
J	293	188	295	193	0,4556	2,7287

As results show, measurements done using compressed air were in most cases near 5 % absolute error taking into consideration the absolute permeability (k_a) and Klinkenberg corrected permeability ($k\infty$) pairs of measurements. And in only two cases were they significant which after re measurement were discarded as human error. Consequently, our suggestion was the alteration of the permeameter to compress air from nitrogen using Sutherland's formula.

3.3. Optimization of liquid permeability measurement protocol

During the laminarity to turbulent measurement, first the original speed was tested and paired with past measurements to assure precision. In all three cases the new measurement is verified with the original values measured in the past. The values in Table 3 present the old and new values measured in 100 ml/h flow rate. After the first measurement the order was as follows 25, 50, 200, 5, 10, 20, 300, finally 400 ml/h. The permeability values are presented in Table 4 while the velocity and pressure gradient values are shown in Figures 3-5. As described previously Darcy's equation can only be applied where the relation between velocity and pressure gradient is linear.

Table 4

Original and newly measured permeability values

Permeability, mD	Sample A	Sample B	Sample C
5ml/h_injection rate	285,6504	172,4678	85,5052
10ml/h_injection rate	275,6974	181,5930	102,7001
20ml/h_injection rate	271,8311	194,5580	99,1388
25ml/h_injection rate	67,5099	102,6594	104,2651
50ml/h_injection rate	127,4449	142,7819	103,5245
100ml/h_injection rate	183,6688	184,3201	102,7830
200ml/h_injection rate	258,9328	212,8676	119,6659
300ml/h_injection rate	264,1225	190,4551	106,9153
400ml/h_injection rate	263,0806	172,7779	102,1984
Divergence from Darcy, %	**Sample A**	**Sample B**	**Sample C**
5ml/h_injection rate	104,2641	116,7713	388,0938
10ml/h_injection rate	109,3979	142,2884	242,0618
20ml/h_injection rate	121,6603	262,5655	27,7291
25ml/h_injection rate	20,3243	3,2025	23,4031
50ml/h_injection rate	22,3935	2,2329	0,0361
100ml/h_injection rate	3,8517	0,3333	8,9033
200ml/h_injection rate	0,6123	0,0163	2,6024
300ml/h_injection rate	14,4137	16,8071	10,0113
400ml/h_injection rate	21,6594	26,9587	14,6353

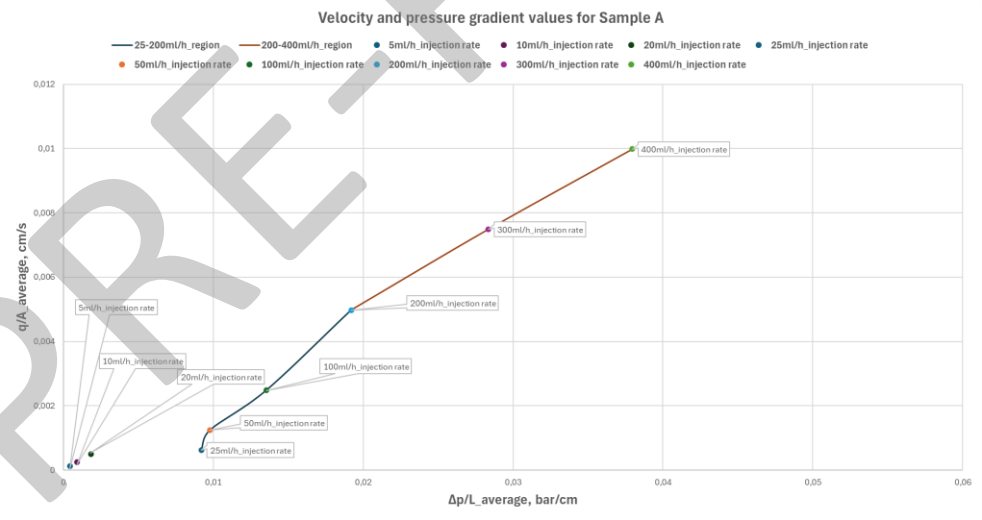

Figure 3

Velocity and pressure gradient values for Sample A

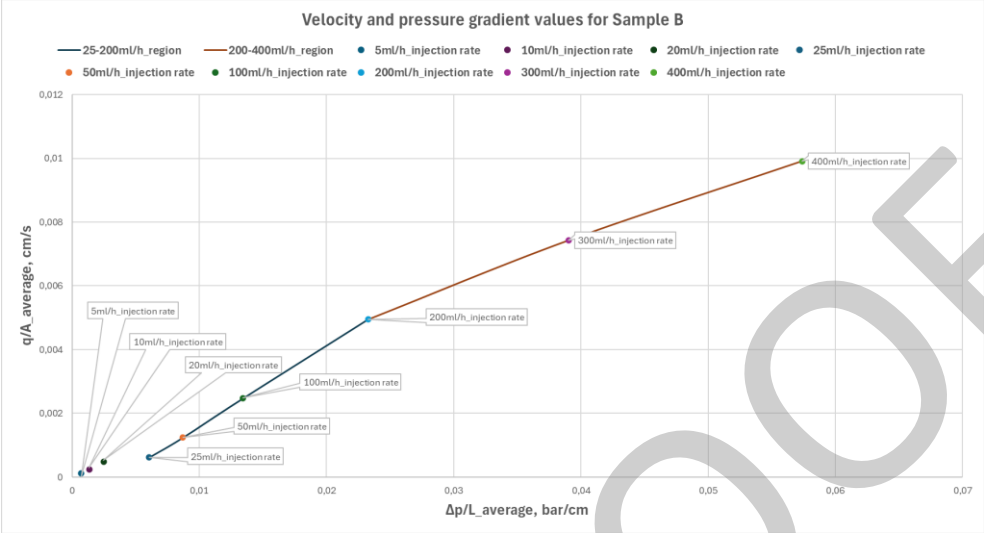

Figure 4
Velocity and pressure gradient values for Sample B

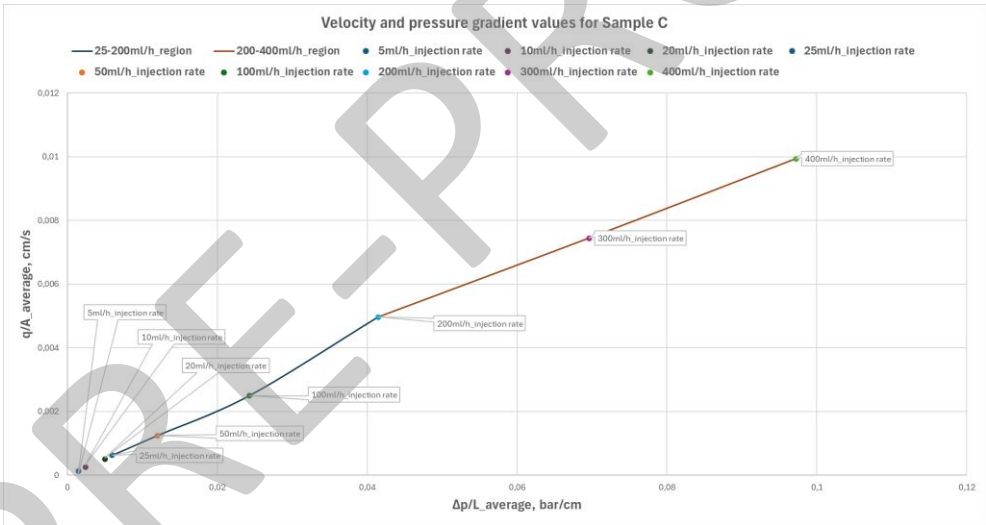

Figure 5
Velocity and pressure gradient values for Sample C

Results show that for all three samples three individual sections were present. At flow rates of 5, 10 and 20 ml/h presumably the so-called pre-Darcy region, at 25, 50, 100, and 200 ml/h the well-developed Darcy region, and covering the 200, 300 and 400 ml/h points deviated from the linear presenting pressure drops higher than those assumed by Darcy's law.

Although at first sight at Sample C the pre-Darcy region did not appear to be present, however, calculating the divergence from the Darcy section showed

otherwise. The pre-Darcy region as many stated is a chaotic flow region in which the pressure drop effects are not yet established. Consequently, we discarded the section in the further analysis. Concentrating only on the linear and post-linear sections.

Numerous researchers have presented that Darcy's law has its limitations and can only be applied for a narrow pressure region where the pressure drop is mainly influenced by viscous forces. These flow conditions are primarily dominant in the reservoir section further from the wellbore area where Darcy's law at the elevated velocity does not apply even if laminar flow conditions are present. This transient preturbulent region is known as the Forchheimer region. Forchheimer's solution (equation 4) by presenting and adding an inertial term to Darcy's equation had proven great correlations not only for the post-Darcy laminar but for the true Darcy region as well (Bagci et al. 2014), (Sedghi and Rahimi, 2011).

The Forchheimer equation is essential in reservoir-scale modeling and field-scale forecasting because it accounts for non-linear flow behavior that becomes significant at high flow velocities, especially in high-permeability formations, near-wellbore regions, and during enhanced recovery operations. Unlike Darcy's law, which assumes purely viscous (linear) flow, the Forchheimer model incorporates inertial effects, providing a more accurate estimation of pressure drops and flow rates under realistic field conditions. Neglecting these non-linearities can lead to underestimation of pressure losses and overprediction of production rates, ultimately reducing the reliability of reservoir performance forecasts and development planning.

Consequently, providing a solution for better estimations for pressure drop estimation at higher fluxes in the porous media while also proving sufficient in the low velocity Darcy region. Consequently, providing a more accurate method for pressure drop calculation at the wellbore sections and for different injections (such as fluid injection; underground gas storage etc.) type processes. We therefore suggested the implementation of the Forchheimer formula to be used instead of Darcy's during the permeability measurement to improve the reliability of the measurements while providing additional information for pressure drops at higher velocities

$$\nabla p = \frac{\mu}{k} v + \beta \rho v^2 \tag{4}$$

In his solution, the pressure gradient equals two pressure drop effects. The first part refers to where the viscous forces dominate (Darcy, laminar linear) and the second where at higher speeds the inertial forces are more dominant (Forchheimer, laminar flow but not linear relations). In the equation β (1/m) is Forchheimer's constant which quantifies how strongly the inertial effects contribute to the pressure loss. And its value changes according to the pore geometry, tortuosity and grain-size distribution of the porous material.

By applying its quadratic form for all speeds except the ones at the pre-Darcy region high correlations were found for all three measured samples (Figure 6-8) where the divergence of values calculated with both cases for the Darcy region was minimal (Table 5).

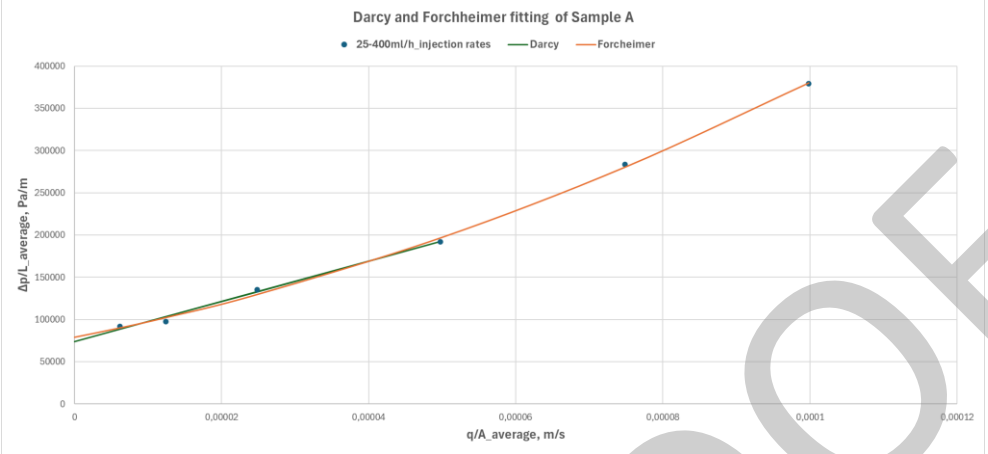

Figure 6
The result of Darcy and Forchheimer fittings for Sample A

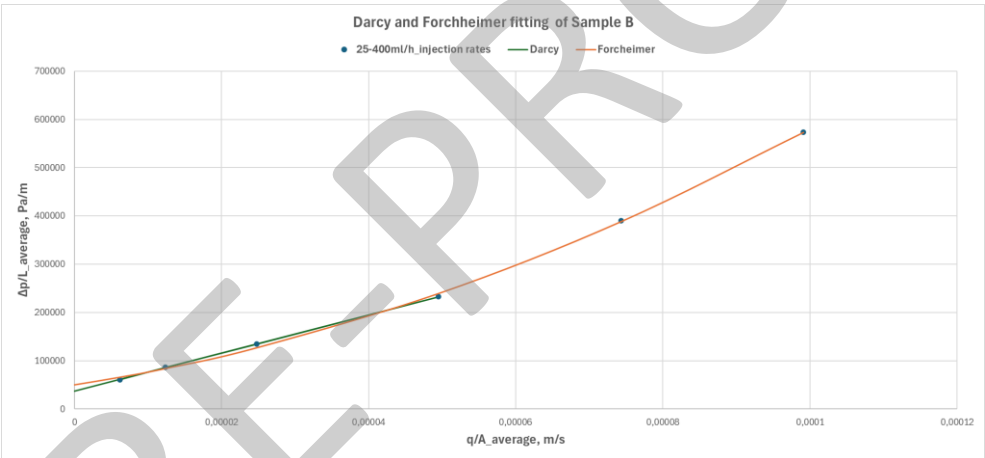

Figure 7
The result of Darcy and Forchheimer fittings for Sample B

Our conclusion after both methods was that the inflexion point was in all cases located at 200 ml/h where the maximum permeability value was measured and belonged to a permeability exceeding the original 100 ml/h value. This marked the true Darcy potential and the beginning of the Forchheimer region for all three selected samples. Also, the original assumption in the past that higher than 100 ml/h speeds would cause turbulent flow was proven false by the excellent regression on Forchheimer's equation.

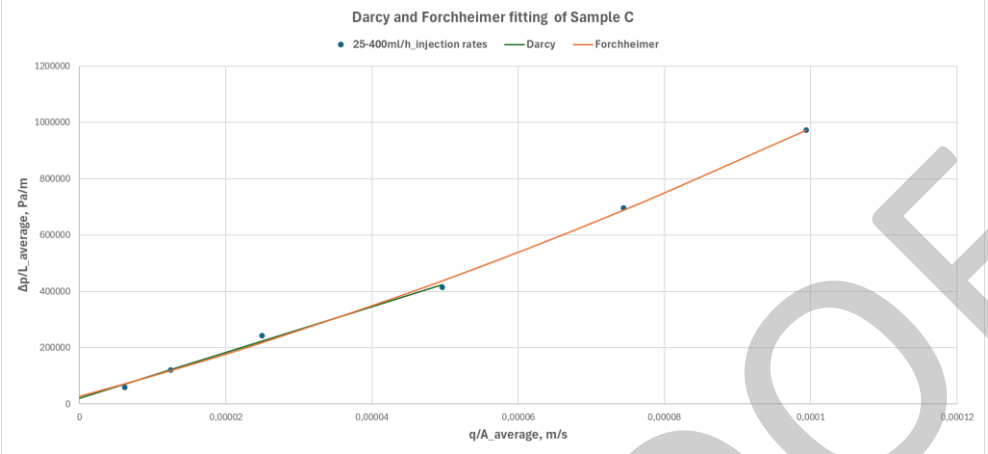

Figure 8
The result of Darcy and Forchheimer fittings for Sample C

Table 5
Divergence in the pressure drop calculated with Darcy and Forchheimer solutions

Solution	**Sample A**	**Sample B**	**Sample C**
Darcy regression	0,9921	0,9998	0,9919
Forchheimer regression	0,9987	0,9993	0,9979
Divergence at the laminar section, %			
25ml/h_injection rate	1,9836	7,6182	1,5690
50ml/h_injection rate	0,8621	2,0243	2,3605
100ml/h_injection rate	2,3631	5,8081	2,1990
200ml/h_injection rate	2,2915	2,9664	3,3134

The significance of this maximum permeability value in reservoir simulation practices is that it presents the lowest pressure gradient obtainable in the pore structure of the sample when fluids are moving on the rim of the wellbore's drainage area.

According to the test data we highly suggest the implementation of a new liquid permeability protocol where the permeability of such porous rock would be measured at multiple rates following the exact order of 50, 100, 200, 300, 400, and 200 ml/h. The second 200 ml/h step should be included to test if any porosity decremental effect had occurred during the higher velocity steps that would permanently damage permeability (Kozhevnikov et al., 2024).

4. Discussion and Conclusions

In this study, we critically evaluated and optimized the porosity and permeability measurement protocols employed in the petrophysical laboratory of the Research Institute of Applied Earth Sciences, with a focus on enhancing their relevance and reliability in the context of modern hydrocarbon reservoir characterization.

While the existing protocols aligned broadly with current standards, we identified key areas—specifically in pore-size distribution analysis, gas dynamic viscosity calculation, and pressure drop estimation—where targeted methodological refinements led to measurable improvements in accuracy. These improvements directly impact the precision of reservoir property assessments, such as fluid flow behavior and storage capacity, which are critical for reliable reservoir modeling and production forecasting.

Importantly, these enhancements were achieved without additional capital investment, by maximizing the capabilities of existing laboratory infrastructure. This demonstrates that even mature measurement workflows can yield significant performance gains when subjected to focused scientific scrutiny, ultimately contributing to more robust and cost-effective hydrocarbon reservoir evaluation.

ACKNOWLEDGMENTS

Supported by the university research scholarship program of the Ministry for Culture and Innovation from the source of the national research, development and innovation fund.

REFERENCES

Anovitz, L. M. & Cole, D. R., 2015. Characterization and analysis of porosity and pore structures. *Reviews in Mineralogy and Geochemistry,* January, Volume Vol. 80, pp. 61-164.

API, 1998. *Recommended Practices for Core Analysis RP 40 II.,* Washington D.C.: API Publishing Services.

Bagci, Ö., Dukhan, N. & Özdemir, M., 2014. Flow regimes in packed beds of spheres from pre-Darcy to turbulent. *Transport in Porous Media,* Volume 104, pp. 501-520.

Dócs, R. et al., 2025. Injection pressure dependence of the permeability of porous rocks measured with incompressible fluid. *International Journal of Engineering and Management Sciences.*

Dócs, R. & Szunyog, I., 2024. Direct porosity measurement using single chamber gas pycnometers. *Geosciences and Engineering,* 12(2), pp. 45-56.

Dotson, B. J., Slobod, R. L., McCreery, P. N. & Spurlock, J. W., 1951. Porosity-Measurement comparisons by five laboratories. *J Pet Technol,* December, 3(12), pp. 341-346..

Jiang, B., Xiao, Q., Shen, R. & Ding, Z., 2024. A new derivation for the apparent permeability model applied to the full Knudsen number range. *Transport in Porous Media,* Volume 151, pp. 2241-2263.

Jimmy, X. L., Reza, R., Tobias, M. M. & Mohammad, S., 2020. Pore size distribution controls dynamic permeability. *Geophysical Research Letters,* 48(5).

Kozhevnikov, E. V., Turbakov, M. S., Riabokon, E. P. & Gladkikh, E. A., 2024. Apparent permeability evolution due to colloid migration under cyclic confining pressure: On the example of porous limestone. *Transport in Porous Media,* Volume 151, pp. 263-286.

Lawrence, A. M. & David, C. R., 2015. Characterization and analysis of porosity and pore structures. *Reviews in Mineralogy and Geochemistry,* 80(1), pp. 61-164.

Luffel, D. L. & Howard, W. E., 1988. Reliability of laboratory measurement of porosity in tight gas sands. *SPE Formation Evaluation,* december, 3(4), pp. 705-710..

Moghadam, A. A. & Chalaturnyk, R., 2014. Expansion of the Klinkenberg's slippage equation to low permeability porous media. *International Journal of Coal Geology,* Volume 123, pp. 2-9.

Mohammed, K. S., 2025. *Klinkenberg effect: Laboratory study of the fluid inpedence of rock permeability.* University of Miskolc: s.n.

Rajib, A., Madland, M. V., Fred, B. & Aksel, H., 2012. *A study of sulphite ions-effects on aging and imbibition capillary pressure curve.* Aberdeen, s.n.

Rapajic, I., Simic, S. & Süli, E., 2025. Modeling capillary rise with slip boundary condition: Well-posedness and long-time dynamics of solutions to Washburn's equation. *Physica D: Nonlinear Phenomean,* Volume 481.

Sedghi, A. M. & Rahimi, H., 2011. Adoption of Manning's equation to 1D non-Darcy flow problems. *Journal of Hydraulic Research,* 49(6), pp. 814-817.

Singh, K., Camulli, H. & Bradley, J., 2024. Sediment size efects on non-Darcy fow: insights from Izbash equation and Forcheimer inertial coefficient analysis. *Hydrogeology Journa,* Volume 32, pp. 1853-1871.

Tanikawa, W. & Shimamoto, T., 2009. Comparison of Klinkenberg-corrected gas permeability and water permeability in sedimentary rocks. *International Journal of Rock Mechanics & Mining Sciences,* 46(2), pp. 229-238.